Energy Saving Potentials of a Photovoltaic Assisted Heat Pump for Hybrid Building Heating System via Optimal Control

Authors

Ettore Zanetti (1), Marcello Aprile (1), Dongsuk Kum (*)(2), Rossano Scoccia (1), Mario Motta (1)

(1) Department of Energy, Politecnico di Milano, 20156 Milano, Italy

(2) Department of The Cho Chun Shik Graduate School for Green Transportation, KAIST, Republic of Korea

Abstract

The recent rise of renewable energy technologies in the building sector is expected to reduce fossil fuel consumption but leads to a greater complexity in the design and control of Heating, Ventilation, and Air Conditioning (HVAC) systems. As a consequence, the traditional control approach does not fully exploit the potential of the photovoltaic-assisted hybrid HVACs. This paper presents an investigation on the energy cost savings and the optimal control strategies of a photovoltaic-assisted hybrid heating system based on optimal control theory. The considered system consists of a radiant floor heating system, a gas boiler and a photovoltaic-assisted air-source heat pump (AS-HP) as heat sources, with a water tank as thermal energy storage (TES). The building thermal dynamics and all the components of the heating system were modelled in MATLAB environment together with a baseline rule-based controller (RBC). The optimal control problem is formulated such that cost function, constraints, state and control variables are defined. Due to a large number of states and control variables, the optimal control problem is converted to the nonlinear parameter optimization problem, and the solution is obtained by using nonlinear programming (NLP). For simulation settings, model parameters, weather, and energy demand profiles were adopted from historical data from a North Italian case study. The simulation results show that the photovoltaic-assisted hybrid heating system coupled with optimal energy management strategy can potentially save up to 20% of the energy consumption cost when compared to the state-of-art RBC and increase the photovoltaic self-consumption by 30%.

Keywords

Optimal control, Hybrid heating system, Thermal storage, Solar assisted air source heat pump.

Nomenclature

T	Temperature (°C)	H	Hot node in the tank
$\dot{m}$	Mass flow rate (kg/s)	M	Middle node in the tank
$\dot{Q}$	Heat transfer rate (kW)	C	Cold node in the tank
P	Power (kW)	*cond*	Conductive
G	Thermal conductance (kW/K)	*inv*	Inverter
U	Global heat exchange coefficient (kW/m^2)	*BOS*	Balance of system
C	Thermal capacity (kJ/K)	*dem*	Demand
c	Specific heat (kJ/KgK)	*en*	Energy cost function
A	Area (m^2)	*dis*	Discomfort cost function
c	Vertical distance TES (m)	*el*	Electric
p	Price (€/kWh)	*build*	Building
R^2	Coefficient of Determination	$feed_{in}$	Subsidy for photovoltaic power sold to grid
k	Optimization parameter	*tot*	Total
W	Optimization weight (€/Kh^2)	*mix*	Adiabatic mixing
h	Hours (h)	*noct*	Nominal operating cell temperature
a_i	Interpolating coefficients (-)	*th*	Thermal storage
		in,out	Inlet, Outlet
Greek symbols		+,-	Only Positive/Negative values
φ	heat transfer rate (kW/m^2)		
η	Efficiency	*Abbreviation*	
Δ	Difference	COP	Coefficient of Performance (kW_{th}/kW_{el})
		OCP	Optimal Control Problem
		CNLP	Constrained Non-Linear Optimization
Subscripts		RES	Renewable Energy Sources
hp	Air source heat pump	RBC	Rule Based Controller
cb	Condensing boiler	AS-HP	Air Source Heat Pump
o	Occupation	PVs	PhotoVoltaic System
s	Solar	R-C	Resistance-Conductance electrical circuit
r	Room	HVAC	Heating, Ventilation and Air Conditioning
w	External wall	SCF	Self-Consumption Factor
f	Floor	MPC	Model Predictive Control
fh	Floor heating	DP	Dynamic Programming
ext	External environment	nZEB	nearly Zero Energy Building
w	Water	CO_2	Carbon Dioxide
PVs	Photovoltaic System	PMP	Pontryagin's Minimum Principle

1. Introduction

1.1 General background

The increasing attention towards environmental issues is driving a fast evolution of green technologies and policies. Residential and commercial buildings account for around the 40% of the total primary energy

consumption [1] , 76% of which goes towards the Heating, Ventilation and Air Conditioning system (HVAC) in the EU [2]. Therefore, a lot of effort has been put to improve the performance of HVACs and reduce their energy consumption and CO_2 emissions while improving the thermal comfort for the people inside the building. However, reducing the consumption of traditional HVAC systems is not enough to reduce the building's energy footprint. In fact, new concepts are rising such as the Nearly Zero Energy Building (nZEB) [3]. Although an official definition of nZEB is not available in the literature [3]-[4], some attempts are present as in [5] and the underlying concept is that nZEBs must use energy efficient technologies to reduce the energy demand and generate enough thermal and/or electrical energy from RES to fulfill the energy demand, so that the overall energy balance is close to zero, an example of the possible technologies is shown in Figure 1.

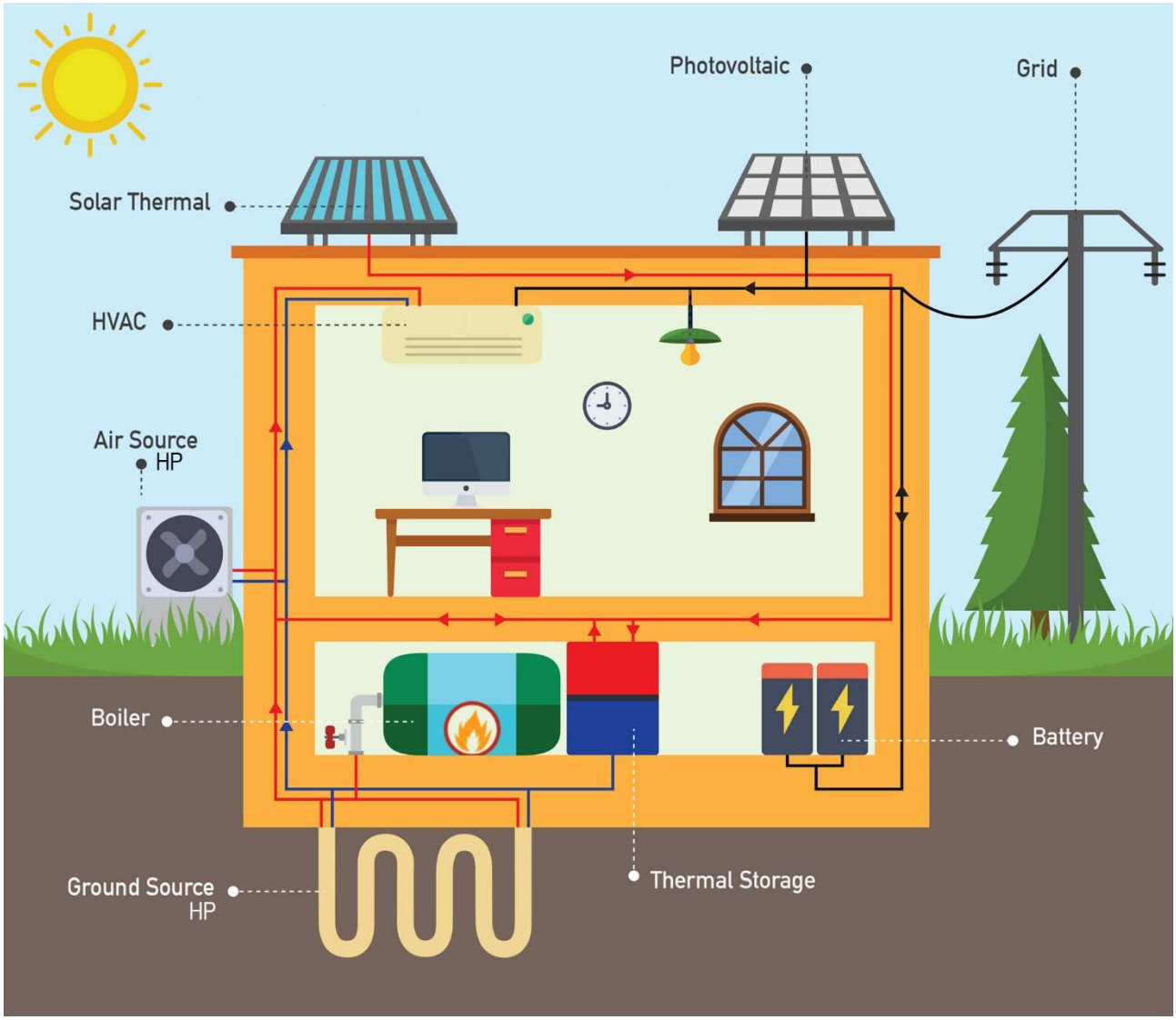

Figure 1 Possible energy configurations for nZEB

Even though a real nZEB is not economically viable yet due to economic and technical issues, there has been an increasing effort to combine newly constructed or renovated buildings with RES and efficient energy conversion technologies such as heat pumps to reduce the building energy footprint [6],[7]. However, to fully exploit the potential of more efficient HVACs a traditional RBC is not enough, because heat pumps and RES performances are affected by weather conditions, causing the RBC tuning process to be challenging. Therefore, the improvement given by the predictive approach might be enough to make it economically viable.

1.2 Hybrid Building Heating System Powered by Photovoltaic Assisted Heat Pump

The building considered in this study is a primary school in North Italy is located close to the Milan area. It consists of four classrooms, a cafeteria and a big hall in the center of the building.

To get close to the nZEB concept, the layout of the heating system includes a gas boiler and a photovoltaic assisted Air Source Heat pump (AS-HP) as heat sources, with a water tank as Thermal Energy Storage (TES): an AS-HP with a heating capacity of 40 kW, since it is the most diffused technology currently in Italy.

A gas boiler with a heating capacity of 40 kW was used as economic reference performance for the AS-HP to check which one is the most economic option in terms of operational cost accounting for the weather conditions, since the AS-HP Coefficient of Performance (COP) is highly dependent on the external temperature and for the North Italian price of natural gas and electricity.

A water tank with the capacity of around 6 000 l was used as TES, because the focus of this work is to consider building retrofitting and this is one of the most economically viable options, furthermore the TES allows the heat source to be decoupled from the building energy demand, giving the Optimal Controller more room for optimization.

Lastly, a photovoltaic system with a nominal output power of 35 kW was chosen, by exploiting all the available surface on the building's roof. The reason behind this specific renewable over the other possibilities is that in Italy PVs have seen a rapid increase in installed in the last decade, thanks to subsidies [7-8] and cost reduction of the technology [10]. Furthermore, no battery system is considered in this case, since the PVs is not over dimensioned with respect to the electric demand and the building is occupied

mainly during the day when the PV production peaks., In case of overproduction from the PVs the excess electricity can be converted in thermal energy with the AS-HP and stored in the TES or sold to the grid.

In Figure 2 a scheme of the whole system is shown.

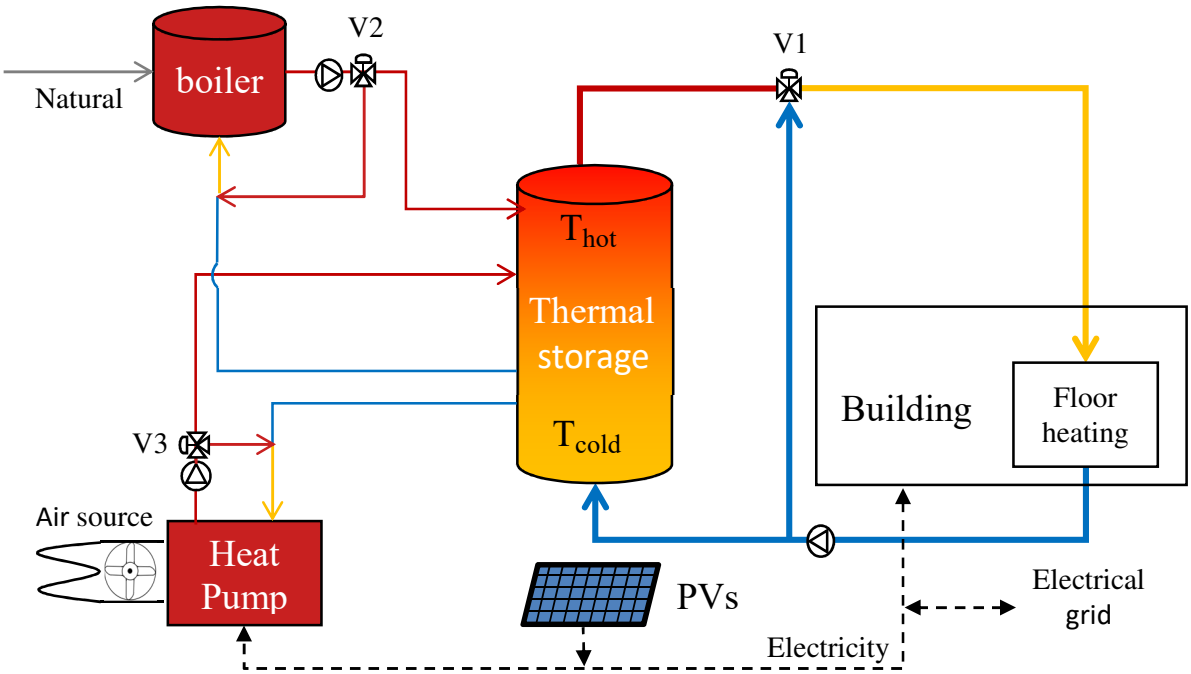

Figure 2 Overall system configuration

1.3 Related works

Plenty of works have been published considering dynamic simulations and experimental studies of hybrid heating systems for space heating and domestic hot water production, where the necessity of an auxiliary heat source is highlighted because the AS-HP cannot be dimensioned for the peak demand due to low efficiency or inability to operate as shown in [11], [12] and [13]. However in [8] and [13] a properly tuned rule based control was used to determine which heating device to operate, in [7] a control approach based on economic optimization was used. If the final objective would be a close to nZEB building increasing the efficiency and economy of the heating system is not enough, in fact renewables and thermal storages should be included in the building framework. In [14] is presented a review on manuscripts comparing different control strategies for a photovoltaic assisted AS-HP, beside the different approaches the common point is that to fully exploit the integration between the AS-HP and the PVs advanced control techniques are necessary [15], and Model Predictive Control (MPC) is among these. Several simulation studies have been

published on MPC applied to systems coupling traditional HVACs with solar energy and hybrid heating systems [16]. In [17], a simulation on a small house in the UK is carried out. Heating is provided by an AS-HP coupled with a solar thermal collector through a water tank. According to simulation results, MPC leads to 9% cost savings with respect to an ON-OFF control strategy. As pointed out by the authors, a limitation in the linear model considered by the MPC algorithm did not permit the proper optimization of the AS-HP, whose COP varies nonlinearly with temperature. In [18] and [19], the dynamics associated with the thermal energy storage are addressed by the MPC algorithm, leading to savings higher than 20% with respect to the reference controller. However, the nonlinear effects of the COP are not considered in the cost function formulation.

In [20], an office in West Lafayette, USA, an AS-HP is used as heat source with a Building-Integrated Photvoltaic-Thermal (BIPV/T) system, which can also provide electrical energy, and a water tank as TES. Different simulations were carried out, the longest being from the 1st of February to the 3rd of March, leading to 34.5% energy savings for MPC with respect to a reference controller. However, the water tank model does not account for thermal stratification, which can lead to unrealistic TES temperatures and COP miscalculation. In the mentioned articles, the main objective is to design a possible real-time MPC, therefore the modelling of the single components is simplified to achieve robust problems that can be implemented in real time applications at the loss of more realistic results. While in this work the degree of freedom in controlling the heat pump are the same as they would be in a real machine, allowing for a more realistic estimation of its performance.

1.4 Contribution

The aim of this work is to utilize optimal control theory to find the theoretical limits that will be used as benchmark for further studies, similarly to what was done for the generic HVAC system in [21], on the performance a photovoltaic assisted hybrid heating system comprising two heat sources, namely AS-HP, a condensing gas boiler, and a water tank as TES, to provide space heating to a school in North Italy, while minimizing the overall energy cost, ensuring thermal comfort and maximizing the photovoltaic self-consumption.

An offline optimization allows to account for COP nonlinearities in the system modeling and the cost function formulation, and to have a more realistic thermal behavior of the AS-HP and the water tank, with

more insights on their optimal control trajectories when coupled with the photovoltaic system. In fact, the main objectives of this work are**:**

- Development of suitable simulation models for the optimization of the hybrid heating system including the air source heat pump, the boiler, the thermal storage and the photovoltaic system.
- Development of a nonlinear optimization problem formulation for the system which accounts for the heat pump nonlinearities.
- Analyze the performance of the hybrid heating system from an economic point of view comparing the results of the Optimal Control Problem (OCP) vs the RBC.
- The article emphasize the increasing importance of including renewable energies into the advanced control framework promoting self-consumption to achieve a nearly zero energy building (nZEB), in fact optimal control allows self-consumption to pass from 67% to higher than 95% for the period considered.

The work flow of the paper will be to find a suitable analytical model for the overall system, define the OCP and the numerical methods to solve it, define the reference RBC and finally compare the results between them.

2. Modelling of the PV-assisted Hybrid Heating System

The first step when dealing with optimal control problems is to define the physical equations governing the dynamics of the system. However, there are limitations on the level of accuracy, in fact there is a tradeoff between the number of dynamic states describing the behavior of the system and the computational time required to find the optimal solution for the problem as discussed in [22].

In this work, given the assumption of an offline optimization, a reasonable model for all the components of the building was considered to represent the general thermal dynamics of the building, including the nonlinearities.

2.1 Thermal Dynamics of the Building

There are many different approaches with different levels of accuracy [23], ranging from dynamic simulations accounting perfectly for the thermal behavior of each room in the building, as in TRNSYS [24] and EnergyPlus [25], that require extensive knowledge of the physical properties of the system, to data

driven low order models able to represent just the global behavior of the building without any physical meaning behind, which are better suited for cases when little to no information is known about the system. For this application a grey-box model with electrical Resistance Capacitance (R-C) electric circuit analogy was used [26] as shown in Figure 3, because not enough data on the building were available to generate a detailed physical model. Furthermore, with this approach the building model results in a set of ordinary differential equations, which lowers the computational time of the simulation with respect to a complex physical model, while maintaining similar results for the required outputs, the room temperature, the energy needs and the outlet temperature from the floor heating system.

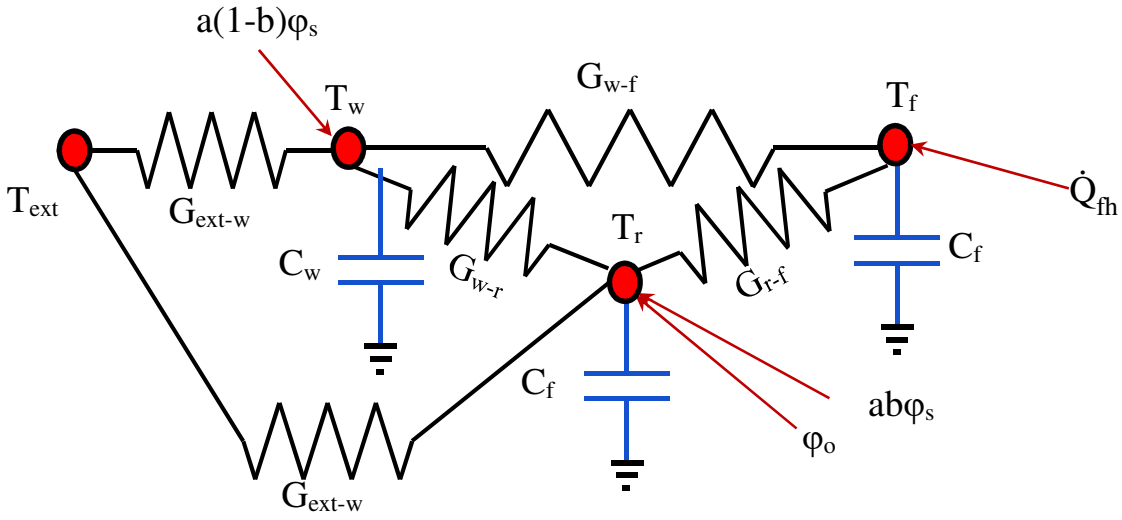

Figure 3 Building lumped parameters scheme

The model has one controllable input $\dot{Q}_{fh}$,the heat rate of water flowing in the floor heating system. Three non-controllable inputs, which are solar irradiance φ_s, occupation heat rate φ_o and the external temperature T_{ext}.

There are three state variables, namely, room temperature T_r, floor temperature T_f and walls temperature T_w. Each state variable has a heat capacity, namely C_r, C_f and C_w. Finally, each G_{xy} represents the thermal conductance between temperatures T_x and T_y.

φ_s is split by the parameter ***b*** between T_w and T_r. The parameter ***a*** instead takes into account the average shadowing and inclination of the sun during the day.

$$\dot{Q}_{fh} = \dot{m}_{fh} c_w \left(T_{fh,in} - T_{fh,out}\right) \quad (1)$$

$\dot{m}_{fh}$(kg/s) is the mass flow rate in the floor heating system, c_w (kJ/kgK) is the water specific heat, $T_{fh,in}$ (°C) is the inlet temperature and $T_{fh,out}$ (°C) is the outlet temperature from the building.

$\dot{m}_{fh}$ and $T_{fh,in}$ are calculated from the mass and energy balance at the recirculation valve V1 in Figure 2, while $T_{fh,out}$ is calculated in the following way:

$$T_{fh,out} = \alpha \cdot T_{fh,in} + (1-\alpha) \cdot T_f \qquad 0 < \alpha < 1 \quad (2)$$

The parameter α can be interpreted as an average heat transfer coefficient between the pipes and the floor.

$$C_f \frac{dT_f}{dt} = -\left(G_{fr} + G_{fw} + \dot{m}_{fh} c_W (1-\alpha)\right) T_f + G_{fr} T_r + G_{fw} T_w + \dot{m}_{fh} c_W (1-\alpha) T_{fh,in} \quad (3)$$

$$C_r \frac{dT_r}{dt} = -\left(G_{rf} + G_{rw} + G_{rext}\right) T_r + G_{rf} T_f + G_{rw} T_w + \varphi_o + ab\varphi_s + G_{rext} T_{ext} \quad (4)$$

$$C_w \frac{dT_w}{dt} = -\left(G_{wf} + G_{wf} + G_{wext}\right) T_w + G_{wf} T_f + G_{wr} T_r + a(1-b)\varphi_s + G_{wext} T_{ext} \quad (5)$$

The final equations of the three nodes model are reported below:

The model was trained using data from January and tested using data from March leading to a R^2 of 0.92 for the average room temperature and R^2 of 0.99 for the $T_{fh,out}$. More details on how the model was derived and the related equations are reported in [26].

The values for the solar contribution are reported in Figure 6, which are historical averaged values for five days from Thursday to Monday for each month of the heating season taken from Arpa Lombardia [27] in the years 2016-2017.

The heat rate according to the occupancy profile is based on a constant heat production coefficient per person according to the ISO 7730 for a total value of 3.8 kW, during working days from 7:20 A.M. to 5.20 P.M.

2.2 Electrical Energy Balance

In the cost function for the optimization problem in Section 4.2 appears the net electrical consumption of the building accounting for the consumption of lights, internal equipment, heat pump and the production of

189 the PVs. The electrical configuration in Figure 4 results trivial considering a steady state operation of the
190 electrical components.

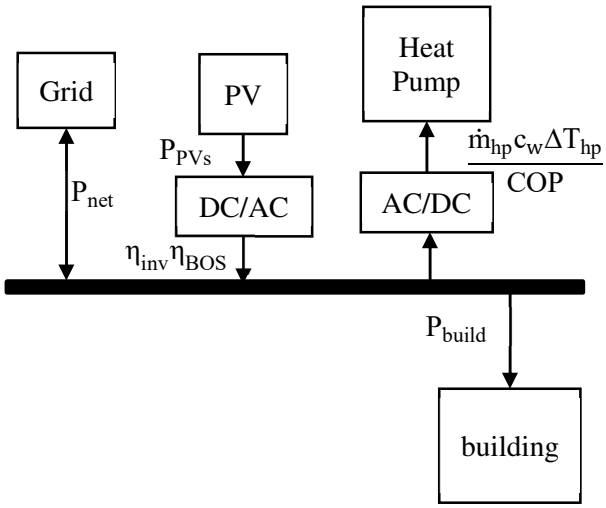

191

192 Figure 4 Electrical configuration

193 Doing the steady-state electrical balance P_{net} is obtained:

$$P_{net} = \frac{\dot{m}_{hp} c_w \Delta T_{hp}}{COP} + P_{build} - \eta_{inv}\eta_{BOS} P_{PVs} \quad (6)$$

194 Where the first term of the equation is the electrical power used by the air-source heat pump while P_{build}
195 is due to the lights and appliances in the building which is modelled after a monitoring done on real primary
196 schools in North Italy [28] on a monthly basis. The monitored P_{build} was multiplied by the volumetric ratio
197 between the considered primary school and the primary school in the reference [28] to account for the size
198 and energy consumption difference between them, obtaining the profiles plotted in Figure 5.

199 The third term is the power generated by the photovoltaic system multiplied by an average value of the
200 inverter and balance of system efficiencies $\eta_{inv}\eta_{BOS}$=0.85.

201 Below are reported the electrical load profile Figure 5 and solar irradiation profile Figure 6:

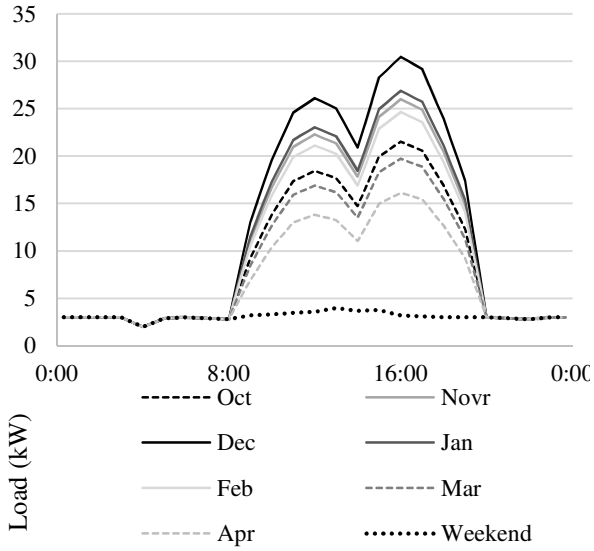

Figure 5 Daily building energy demand for each month

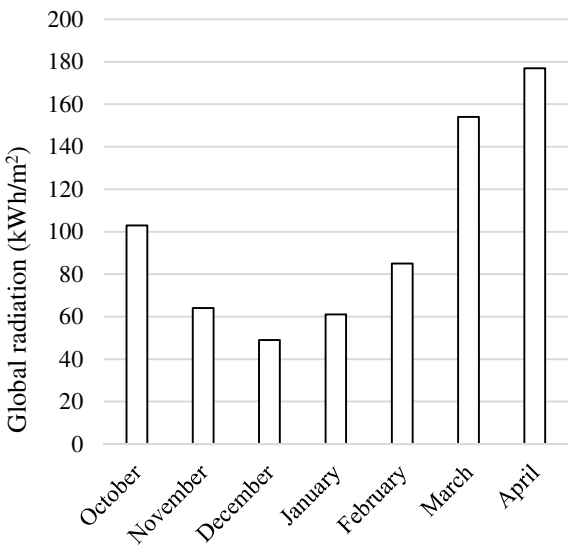

Figure 6 Average monthly radiation

202

203 The reason behind the specific electrical profile shown in Figure 5 is due to the fact that lunchtime in Italian
204 schools is between 12:30 P.M and 1:30 P.M., during which employees and students go to lunch and may
205 switch off their appliances.

206

207 **2.3 Thermal Energy Storage (TES) Water Tank**

208 A common way to model a water tank TES is by using a multi-node stratified approach [29].

Each ith node represents a mass of water at constant temperature and increasing the number of nodes allows to have a more accurate representation of the temperature profile inside the tank. In [29], different numbers for the nodes were tried showing that the lower the number of nodes the higher the thermal inertia associated

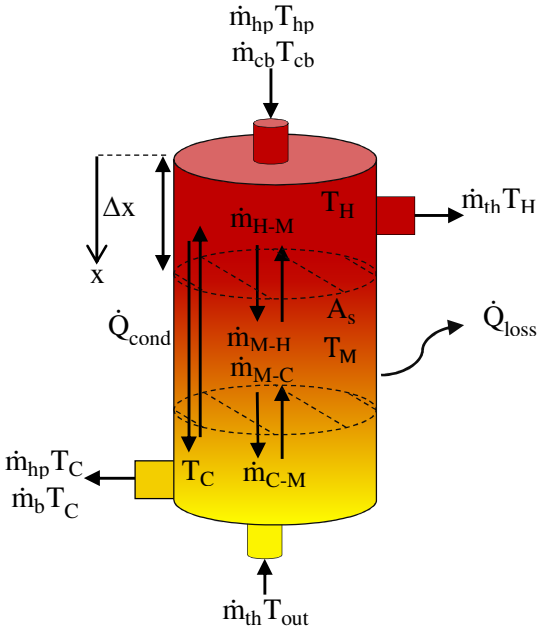

to the single node. This leads to a mismatch between the predicted and the real temperature in case of large gradients in the TES. In this work space heating is considered where the temperature range is small, therefore an appropriate three nodes model has been developed. In Figure 7 the scheme is reported:

Figure 7 water tank TES scheme

T_H, T_M and T_C are respectively, the hot temperature node, the medium temperature node and the cold temperature node, while $\dot{m}_{i\text{-}j}$ are the water mass flow rate between the nodes to compensate for the overall mass balance of the water tank. $\dot{m}_{hp}$ and $\dot{m}_b$ are respectively the heat pump and the boiler water mass flow rates in the thermal storage, while T_{hp} and T_{cb} are the respective inlet temperatures.

$\dot{m}_{th}$ is the mass flow rate from the thermal storage to the building and T_H is the outlet temperature towards the building while $T_{fh,out}$ the return temperature from the building floor heating pipes.

$\dot{Q}_{loss}$, in Eq. (7), is the heat rate loss towards the environment and simply calculated as a global heat transfer coefficient U times the external area A_x of each node and the temperature difference between the node and the external temperature considered as constant. $\dot{Q}_{cond}$ is the conductive heat transfer between the

nodes, which is the temperature difference between the nodes divided by Δx which is the distance between the nodes and multiplied by the cross-sectional A_s and water thermal conductivity λ, the resulting equations for the nodes are reported below:

$$\dot{Q}_{loss} = UA_x(T_{ext} - T_i) \tag{7}$$

$$\dot{Q}_{cond} = \frac{k}{\Delta x} A_s(T_i - T_j) \tag{8}$$

$$C_H \frac{dT_H}{dt} = \dot{m}_{hp} c_W T_{hp} + \dot{m}_{cb} c_W T_{cb} - \dot{m}_{th} c_W T_H + \dot{Q}_{cond} + \dot{Q}_{loss} + \dot{m}_{H-M} c_W \left(T_H\left(1 - f_{th_{H-M}}\right) + T_M f_{th_{H-M}}\right) \tag{9}$$

$$C_M \frac{dT_M}{dt} = \dot{m}_{M-H} c_W \left(T_M\left(1 - f_{th_{M-H}}\right) + T_H f_{th_{M-H}}\right) + \dot{m}_{M-C} c_W \left(T_M\left(1 - f_{th_{M-C}}\right) + T_C f_{th_{M-C}}\right) + \dot{Q}_{cond} + \dot{Q}_{loss} \tag{10}$$

$$C_C \frac{dT_C}{dt} = \dot{m}_{th} c_W T_{fh,out} - (\dot{m}_{hp} + \dot{m}_{cb}) c_W T_C + \dot{Q}_{cond} + \dot{Q}_{loss} + \dot{m}_{C-M} c_W \left(T_C\left(1 - f_{th_{C-M}}\right) + T_M f_{th_{C-M}}\right) \tag{11}$$

The last parameter to consider in the nodes equations is f_{th},described by Eq. (12), that determines the direction of the flow in the water tank TES depending on mass flow rate balance of the water tank. When the TES is charging the water flows from the hot node to the cold and vice versa. To describe this behavior without using a bilinear function a hyperbolic tangent shape function has been adopted.

$$f_{th_{i-j}} = \frac{1 + tanh\left(C_i e \dot{m}_{i-j}\right)}{2} \tag{12}$$

C_i is a constant value multiplied by the Euler number e, in this way $f_{th\_\,i\text{-}j} = 1$ when the TES is charging and $f_{th\_\,i\text{-}j} = 0$ when it is discharging.

2.4 Air-source Heat Pump

The heat pump is a key component of the heating system, and therefore its behavior should be modeled as close as possible to reality. In principle, two aspects of the heat pump behavior at different operating temperatures shall be considered: full load heating capacity and COP. However, to simplify the implementation of the control algorithm, a constant full load heating capacity is assumed, based on the

consideration that, when a storage is present in the system, the approximation introduced here does not have an important effect on the overall energy performance of the heat pump.

Therefore, the main parameter becomes the COP of the heat pump, which is mainly a complex function of the external temperature T_{ext} and T_{hp} the feed temperature to the TES. The COP expression, Eq.(13), was derived by interpolating the performance data from a manufacturer's catalogue for a 40 (kW) heating capacity air-source heat pump, with a three digits polynomial function of the two variables.

$$COP = COP_0 - a_0 T_{hp} + a_1 T_{hp} - a_2 T_{hp}^2 - a_3 T_{hp} T_{ext} + a_4 T_{ext}^2 - a_5 T_{hp}^3 + a_6 T_{hp}^2 T_{ext} - a_7 T_{hp} T_{ext}^2 - a_8 T_{ext}^3 \quad (13)$$

The resulting approximation leads to a R^2=0.99 for the interpolated points. In Table 1 the values of the coefficients are shown:

Table 1 – COP parameters

COP_0	a_0	a_1	a_2	a_3
5.114E+00	4.330E-02	2.073E-01	1.150E-03	3.298E-03
a_4	a_5	a_6	a_7	a_8
4.773E-03	1.546E-05	1.770E-05	1.834E-05	2.853E-04

2.5 Gas boiler

For the boiler model an average value for the efficiency on the lower heating value (η_{cb} = 0.95) was selected starting from a typical condensation boiler, under the assumption that the efficiency of the boiler does not vary as much as the AS-HP COP with the T_{ext} and the feed temperature T_{cb} considering that it is used for a floor heating in the condensation range.

2.6 Photovoltaic system

The main component of the PV model are the photovoltaic modules, which were chosen with a nominal power of 250 (W). The total nominal power of the PV plant is 35 (kW), sized to fit the peak energy demand of the building lights, internal equipment and heat pump. In Eq. (14) is reported the expression to calculate the resulting PVs power output P_{PVs} calculated according to the Italian standard CEI 82-25 while the numerical values can be found on the manufacturers datasheet.

$$T_{cell} = T_{ext} + \frac{\varphi_s(T_{noct} - T_{ref})}{\varphi_{noct}} \quad (14)$$

$$P_{PVs} = \varphi_s(1 - \gamma(T_{cell} - T_{noct}))\eta_{PVs}A_{PVs}K_{shading} \quad (15)$$

Where T_{cell} is the PVs module's temperature and T_{ref} = 20 (°C) is the environment reference temperature, T_{noct} = 45 (°C) is the nominal operating temperature and φ_{noct} = 800 (W/m^2) is the reference radiation. γ is a dimensionless parameter that determines the performance loss when $T_{cell}>T_{noct}$, η_{PVs}=0.157 is the module nominal efficiency, A_{PVs}=220 (m^2) is the total PVs area and $K_{shading}$=0.95 is the shading factor assuming rural surroundings.

3. Optimal Control Problem and Solution Search Method

3.1 Optimal Control Problem Formulation

Optimal control deals with problems in which time variant inputs controllable $u_i(t)$ are chosen for a dynamic system $x(t)$ such that an optimality criterion is met under certain boundary conditions, constraints $c(t)$ on dynamic states and controls, and time variant non-controllable inputs called disturbances $w(t)$. The criterion is the cost function J associated with the optimal control problem. The general formulation for J can be expressed as in:

$$J = h(x(t_f), t_f) + \int_{t_0}^{t_f} g(x(t), u(t), w(t), t)\, dt \quad (16)$$

Where $g(x(t),u(t),w(t),t)$ is a function of states and controls and $h(x(t_f),t_f)$ is the terminal cost. In Figure 8 a simplified diagram explaining the optimal control problem formulation is shown:

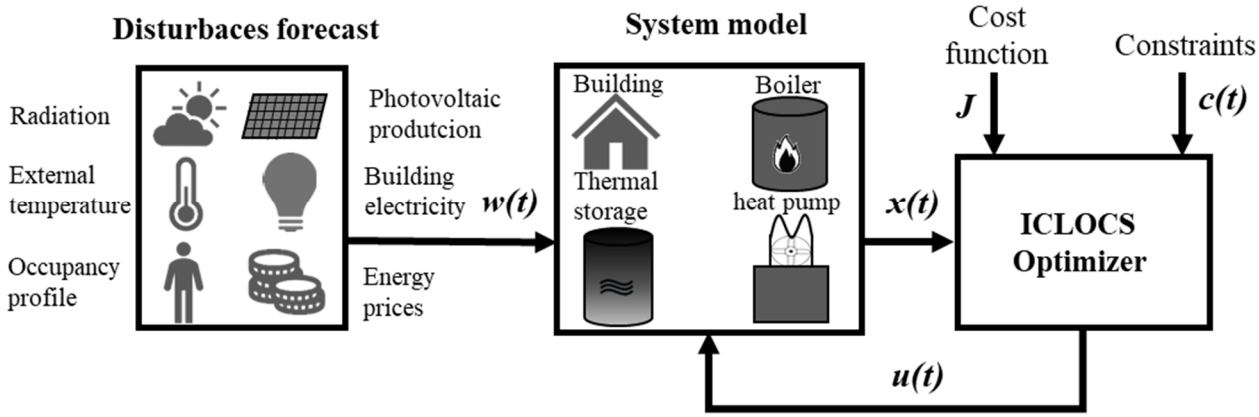

Figure 8 Diagram showing the flow of the optimal control problem formulation

The flow of the optimal control shown in Figure 8 goes from left to right, where the disturbances forecast *w(t)* are applied to the system model together with an estimation of the controls *u(t)* to find the values of the states *x(t)*, which are given together with the cost function and the constraints to the ICLOCS optimizer.

The summary of states *x(t)*, the controls *u(t)*, disturbances *w(t)*, cost, time horizon and constraints present in the actual control problem are reported in Table 2.

Table 2 States, controls and disturbances for the considered problem

Cost (J)	Energy consumption (€) Thermal comfort (K^2h)
Stage (t)	Thursday to Monday (day), Heating season October to April (month)
Controls (u)	$\dot{m}_{th}$ (kg/s):$[0,\dot{m}_{TES_{max}}]$ $\dot{m}_{hp}$ (kg/s): $[0,\dot{m}_{hp_{max}}]$ $\dot{m}_{cb}$ (kg/s):$[0,\dot{m}_{cb_{max}}]$ T_{hp} (°C): $[0,T_{hp_{max}}]$ T_{cb} (°C):$[0,T_{cb_{max}}]$
States (x)	T_f (°C) :[-inf,inf] T_r (°C):[-inf,inf] T_w (°C) :[-inf,inf] T_H (°C):[-inf,45] T_M (°C) :[-inf,45] T_C (°C) :[-inf,45]
Disturbances (w)	T_{ext} (°C) φ_r $(\mathrm{kW/m^2})$ φ_o $(\mathrm{kW/m^2})$ P_{PVs} (kWe) P_{build} (kWe) p_{el}(€/kWh)
Subject to (c)	$0\leq\frac{\dot{m}_{hp}}{\dot{m}_{hp_{max}}}(T_{hp}\text{-}T_C)\leq\Delta T_{hp_{max}}$ $0\leq\frac{\dot{m}_{cb}}{\dot{m}_{cb_{max}}}(T_{hp}\text{-}T_C)\leq\Delta T_{hp_{max}}$ $T_{mix_{t0}}$ (°C)≈$T_{mix_{t0}}$ (°C) defined in (21

3.1.1 Cost function J

The objective of the optimal controller in this problem is to minimize the economic cost of the energy provided to the building while ensuring a minimum level of thermal comfort, given by the temperature difference with respect to the set point, inside the rooms. In [30] is reported a way to put together the energy consumption and the discomfort, by starting from that formulation and adapting it to this case we obtain the total cost function in Equation 17:

$$min\, J_{tot} = \int_{t_0}^{t_f} \left(kJ_{en}(t) + (1-k)J_{dis}(t) + J_{control_i}(t) \right) dt \qquad 0 < k < 1 \tag{17}$$

293 J_{tot} has three contributions, the cost function accounting for energy consumption $J_{en}(t)$ explained
294 in Eq.(18), the cost function accounting for thermal discomfort $J_{dis}(t)$ explained in Eq.(19) and the
295 cost function accounting for the controls' constraints $J_{control_i}(t)$ explained in Eq.(20).
296 $J_{en}(t)$ and $J_{dis}(t)$ are multiplied by k, which is a dimensionless parameter that expresses the relative
297 importance between the energy and the discomfort cost functions. Thus, for $k = 1$, the OCP minimizes only
298 the energy consumption, while for $k = 0$ only the discomfort would be minimized.

$$J_{en}(t) = p_{el}(t) \cdot P_{net}^{+}(t) + p_{feed_{in}} P_{net}^{-}(t) + \frac{p_{ng} \cdot \dot{m}_b(t) c_w \cdot \Delta T_b(t)}{\eta_b} \tag{18}$$

299 The first term represents the maximum between zero and the electrical balance in of the building Eq. (6)
300 multiplied by the price of the electricity p_{el}, the second term represents the minimum between zero and the
301 electrical balance of the building multiplied by the feed-in tariff $p_{feed_{in}}$. The last term represents the boiler
302 power multiplied by the price of natural gas p_{ng}. The prices were derived from the Italian electric grid
303 manager GSE [31], accounting for monthly variation and a day-night shift for the price of electricity.

$$J_{dis}(t) = W \frac{\varphi_o(t)}{\varphi_{o_n}} \left(T_r - T_{ref}\right)^2 \tag{19}$$

304 T_r is the room temperature, $T_{ref} = 21$ (°C) is the room reference temperature, $\frac{\varphi_o(t)}{\varphi_{o_n}}$ is the ratio between the
305 occupancy heat gain rate and its nominal value of 3.8 (kW) and W is a constant weight that converts the units
306 of the discomfort (K^2h) in price units (€).
307 The third contribution considers the start-up and shut-down frequency of the AS-HP and the condensing
308 boiler. It accounts for the wear on the system:

$$J_{control_i}(t) = K_i \left(\frac{1}{2} tanh\left(\left(\frac{du_i}{dt}\right)^2 - \left(\frac{du_{i_0}}{dt}\right)^2 \right) + \frac{1}{2} \right) \left(\frac{du_i}{dt}\right)^2 \tag{20}$$

309 K_i is a constant weight for the specific control input, and $\left(\left(\frac{du_i}{dt}\right)^2 - \left(\frac{du_{i_0}}{dt}\right)^2\right)$ is the difference between
310 the maximum allowed derivative (maximum ON-OFF frequency) and the actual derivative, so that
311 the cost is zero when the derivative is within range and increases the larger the difference between
312 the derivatives.

313 *3.1.2 Stage: period considered and time horizon*

314 For the optimal control problem, the whole heating season in Italy was considered. It starts on the 15th of
315 October and it ends on the 15th of April. For each month five representative days were chosen for the
316 prediction horizon, starting from Thursday to Monday, to account for the Weekend when there are no people
317 in the building.

318 *3.1.3 Controls chosen for the heating system u(t)*

319 There are a total of five control variables in this problem. Flow rate $\dot{m}$ and outlet temperature T_{out} for the
320 heat pump and boiler, to control both $\dot{m}$ and T_{out} a recirculation valve is placed after the heat pump (V3) and
321 after the boiler (V2) as shown in Figure 2. The last control variable is the flow rate from the thermal storage
322 to the building $\dot{m}_{th}$, with which the inlet temperature to the building $T_{fh,in}$ is regulated using the valve (V1).
323 The upper and lower boundaries for the control variables were chosen according to the manufacturer's
324 datasheets.

325 *3.1.4 States of the system x(t)*

326 The states of the system are all the variables that accounts for the dynamics. In this case the three
327 temperatures of the Building, floor T_f, room T_r and walls T_w and the three temperatures of the storage, hot
328 node T_H, medium node T_M and cold node T_C (°C) . There are not upper or lower bounds for the building
329 temperatures, while there is an upper bound at 45 °C for the storage temperatures, since that's the maximum
330 allowed temperature for the floor heating system.

331 *3.1.5 Disturbances of the system w(t)*

332 The disturbances are all the time varying variables that are not controllable, they are explained in the sections
333 above and summarized in Figure 8. Being non controllable, they do not have upper or lower bounds.
334 However, they should be smooth enough in order for the optimizer to handle them.

335 *3.1.6 Constraints of the system w(t)*

336 Beside the upper and lower bounds, there can be constraints on the initial and final states or physical
337 constraints on the system equations as summarized in Table 2. The OCP is designed to keep the final T_{mix,t_f}
338 of the TES closer to the initial T_{mix,t_0}, to approximate that the initial and final energy stored in the TES are
339 equal. Then the other two constraints express the maximum ΔT available to the heat pump and boiler in
340 function of the controls *u(t)* and states *x(t)* chosen for the system.

3.2 Numerical approach to solve the Optimal Control Problem

To solve numerically this optimal control problem many approaches are possible, like: Dynamic Programming (DP), the Pontryagin's Minimum Principle (PMP) or the Constrained Non-Linear Programming (CNLP). Among these the CNLP method has been used in this work.

Although Dynamic programming guarantees the global optimum, it is subjected to Bellman's curse of dimensionality, meaning that the computational time increases exponentially with the number of states in the dynamic system, while Approximate DP solves the curse of dimensionality, but is not trivial to apply constraints on the controls using this approach, find the guesses for parameters which are not physical, and the global optimum is not guaranteed. PMP converts the optimal control problem from the dynamic system, cost function and constraints form into a boundary value problem, with this mathematical formulation is possible to express a necessary condition for optimality on the controls allowing a faster speed convergence with respect to DP, however it presents the same issues as approximate DP on the constraints and global optimality.

So, a CNLP approach was used because even though it is not as accurate as the previous approaches since it does not guarantee the global optimum, it is straightforward to deal with the problem's constraints. There are many ways to convert an optimal control problem into a CNLP problem. ICLOCS [32], a MATLAB [33] based toolbox, is used to convert the optimal control problem into a CNLP problem using a Direct Collocation method with Hermite-Simpson discretization [34], then the resulting CNLP is solved using the Interior Point OPTimizer (IPOPT) [35]. Different time steps were tried, namely 10 min, 20 min and 40 min, the solutions did not present significant difference in the economic results, because the time step is sufficiently small to catch the system dynamics and disturbances variation to optimize the operation of the AS-HP, the boiler and the TES, therefore 40 min was chosen as time step.

3.3 Rule Based Control

The Rule Based Control (RBC) is designed to guarantee thermal comfort during occupied hours and charging the TES. The available measures are the room temperature T_r, which according to the Italian regulation should stay between 20 (°C) and 22 (°C) during the heating season, the external temperature T_{ext}

and the TES adiabatic mixing temperature T_{mix} described in (21 which the operational range is between 20 (°C) and 45 (°C).

$$T_{mix} = \frac{T_H C_H + T_M C_M + T_C C_C}{C_H + C_M + C_C} \quad (21)$$

To control T_r, the inlet temperature in the building's floor heating $T_{fh.in}$ is regulated according to the climatic curve in Figure 9.

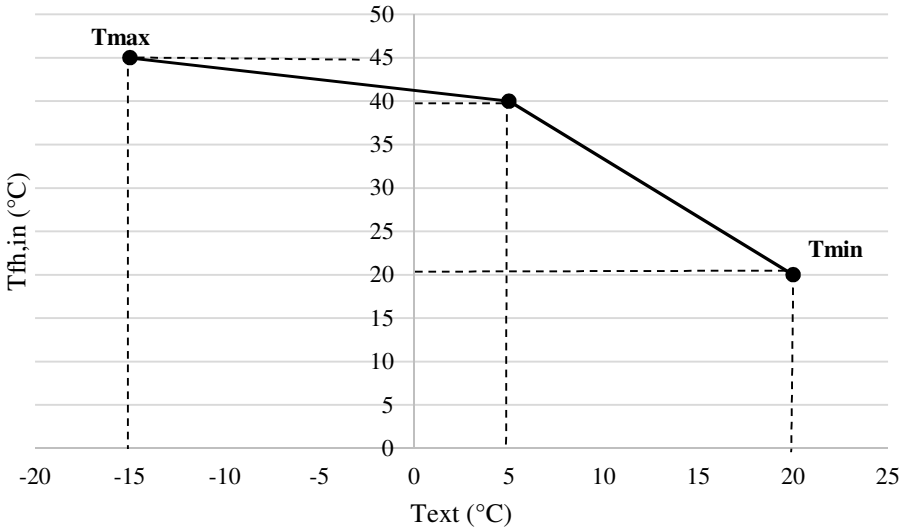

Figure 9 Climatic curve. The inlet temperature in the building floor heating $T_{fh,in}$ is function of the external temperature T_{ext}

To charge the TES, the AS-HP and condensing boiler are used in a sequential ON-OFF operation, meaning that if $T_{mix} < T_{hp\text{-}ON}$,where $T_{hp\text{-}ON} = 40$ (°C) is the TES mixing temperature, only the AS-HP will be used to charge the TES and if $T_{mix} < T_{cb\text{-}ON} < T_{hp\text{-}ON}$ also the condensing boiler will be switched onto charge the TES. The monthly values for $T_{cb\text{-}ON}$ are reported in Table 3. The values of $T_{cb\text{-}ON}$ were taken accounting for the external temperature, so that when it's colder the boiler will start helping out the AS-HP earlier, allowing for a higher average monthly COP.

3.4 RBC simulation settings

In Table 3 are also reported the values for the building set-back temperature $T_{set\text{-}back}$ and the time shifts in hours between the start-up of the floor heating system and the first occupied hour during working days (7:20 A.M.). Shift-work is the time shift for working days and shift-weekend is the time shift for the

weekend before Monday. The values of the time shift presented in Table 3 were carefully chosen for each month via trial-and-error procedure in order to ensure that the temperature inside the building at the start of the days would always be in the comfort band 20-22 (°C).

Table 3 – RBC tuning parameters

	shift-work (h)	**shift-weekend (h)**	**Tset-back (°C)**	**Tcb-ON (°C)**
October	6	11	16.5	31
November	6	11	17	32
December	8	12	18.5	35
January	8	14	18	35
February	7	13	18	34
March	4	11	17	31
April	5	10	16	30

The RBC modeling and simulation has been modelled in MATLAB environment using a 40 (min) time step.

4. Simulation Results

4.1 Economic and comfort performance comparing OCP and RBC results for heating season

In this section, the results for the whole heating season are reported in terms of economic performance, environmental performance and heating system performance comparing the results of the Optimal Control Problem (OCP) and the Rule-Based Controller (RBC).

In Figure 10 the solutions for January and April of the RBC (colored squares) are compared to the OCP solutions (colored dots) varying the parameter k. The energy cost is plotted on the x-axis against the cumulative difference between the room temperature and its reference $\mathrm{T_{ref}} = 21\ ℃$ divided by the occupied hours as shown in Eq.(22).

$$\Delta T_{set-point} = \frac{\sqrt{\int_{t_0}^{t_f} \frac{J_{dis}(t)}{W}}}{h_{occ}} \tag{22}$$

In this way $\Delta T_{set\text{-}point}$ becomes the hourly difference between T_r and T_{ref}, when this value is between zero and one, $0 \leq \Delta T_{set\text{-}point} \leq 1$, the temperature in the room T_r will be between 20 and 22 (°C), $20 \leq T_r \leq 22$ (°C).

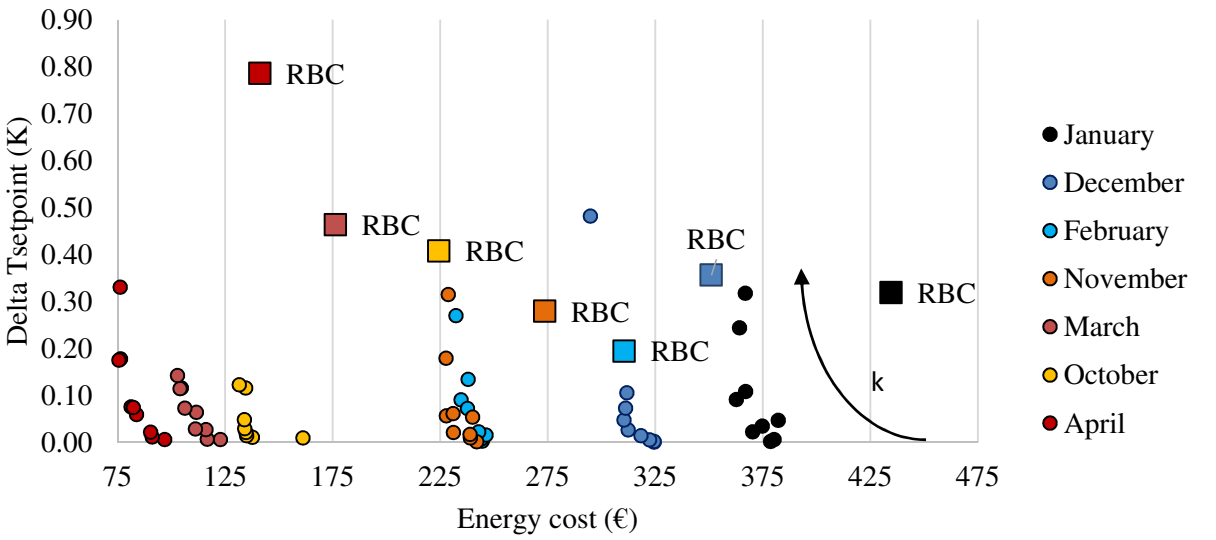

Figure 10 monthly results OCPs vs RBC in terms of energy cost and thermal discomfort for different k values (Dots)

Increasing the value of *k*, increases the economic weight while reducing the set-point error weight in the cost function, since the cost function trend is hyperbolic changing the value of *k* as in [30], after a certain threshold reducing *k* value, thus giving more weight to the energy cost, will only increase the set-point error without reducing the energy cost. This limit value has been considered as the global optimum of the OCP.

In Figure 11 and Figure 12 the economic results and the CO_2 emissions are reported considering only the best solution for the OCP.

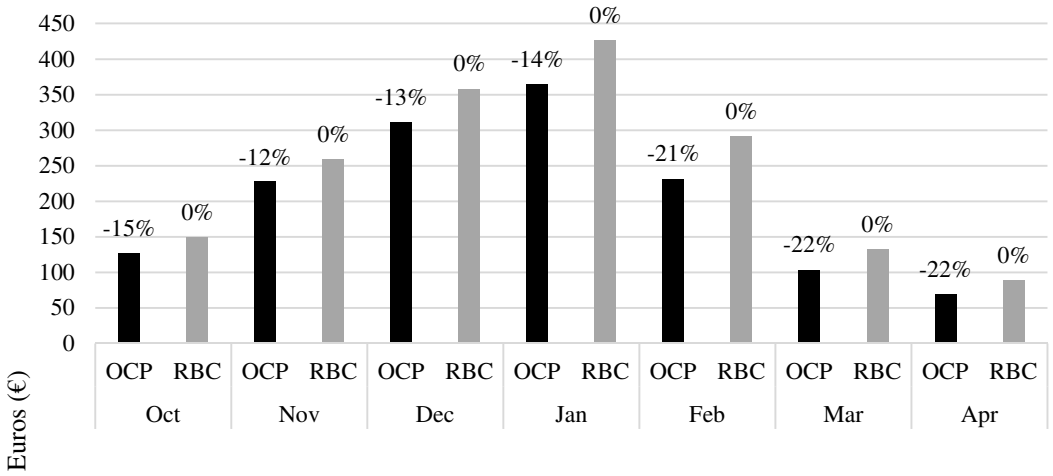

Figure 11 monthly energy cost for space heating: OCPs vs RBC

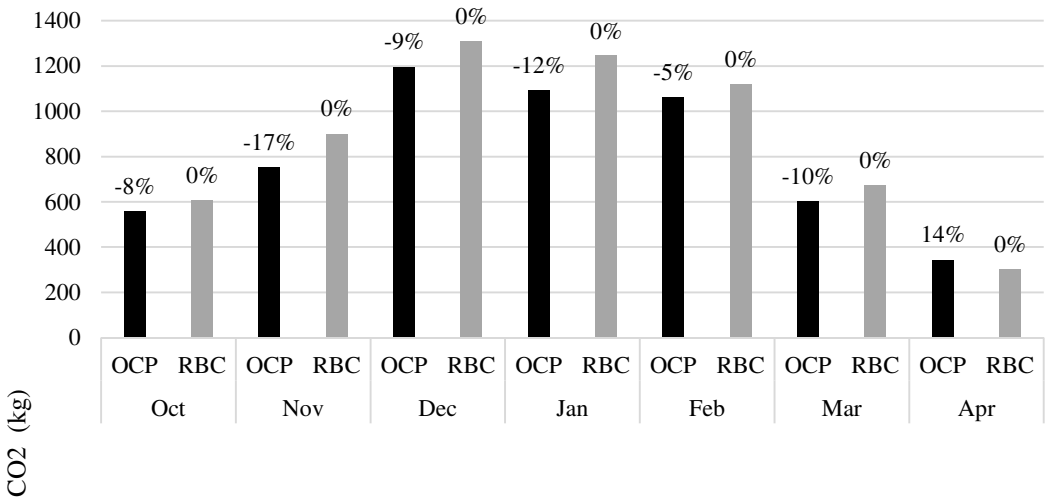

Figure 12 monthly CO_2 emission for space heating: OCPs vs RBC

Considering the two figures, the average economic savings are 18% and the average avoided CO_2 emissions are 10% even though they not directly included into the cost function formulation. The conversion coefficient for the calculation of the CO_2 emissions are reported in Table 4 and valid for Lombardy calculated based on the local grid production mix (source: GSE and Energia Lombardia).

Table 4 monthly CO_2 emissions coefficients for the AS-HP and condensing boiler

	ECO_2 (g/kWh) hp	**ECO_2 (g/kWh) cb**
October	336	200.952
November	313	200.952
December	344	200.952
January	343	200.952
February	344	200.952
March	318	200.952
April	289	200.952

Looking at the coldest months in the previous figures, namely December and January, the economic savings are around the 14%, in Autumn and Spring are savings around the 20%.

The values of Q_{hp} and Q_{cb} for every month are reported in Figure 13. Considering the heat delivered Q_{tot} by the AS-HP and condensing boiler to charge the TES, the difference between the OCP solution and the RBC is 16% for Winter and 4% for Spring-Autumn. However, the production mix is different, in Winter the RBC

mix is 72% Q_{hp} and 28% Q_{cb} while the OCP solution mix is 66% Q_{hp} and 34% Q_{cb}. In Spring-Autumn the RBC mix is 87% Q_{hp} and 13% Q_{cb} while the OCP solution mix is almost 100% Q_{hp}.

As shown with the production mix difference the OCP solution always uses the cheaper option to charge the TES, which can be the condensing boiler in Winter that has a constant efficiency, while in Autumn and Spring it mainly uses the AS-HP, which has a variable COP in function of the external temperature leaving more room for optimization.

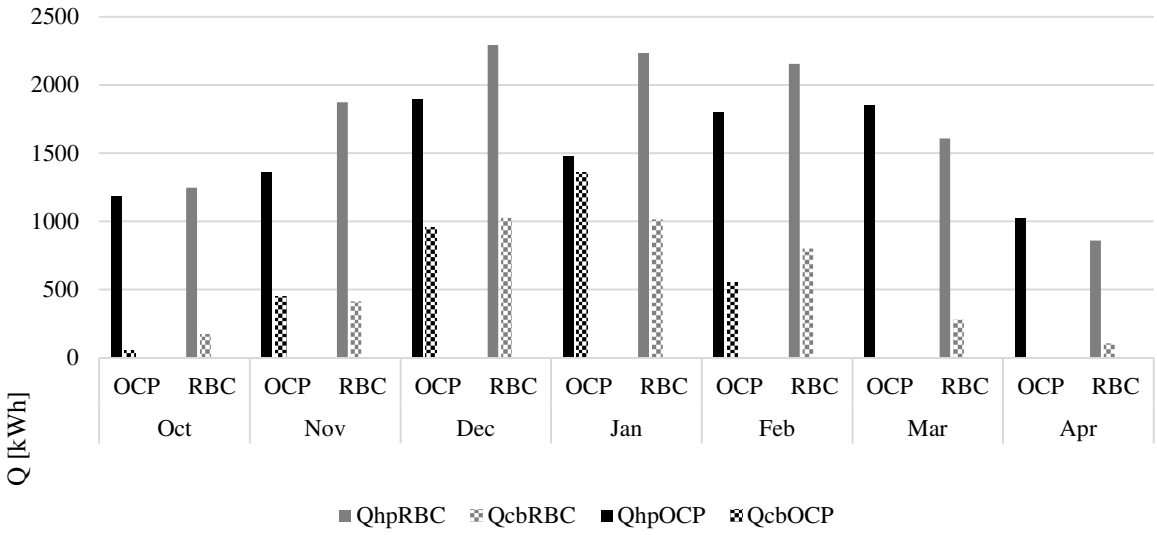

Figure 13 energy delivered to TES, in blue Q_{hp}, in red Q_{cb}: OCPs vs RBC

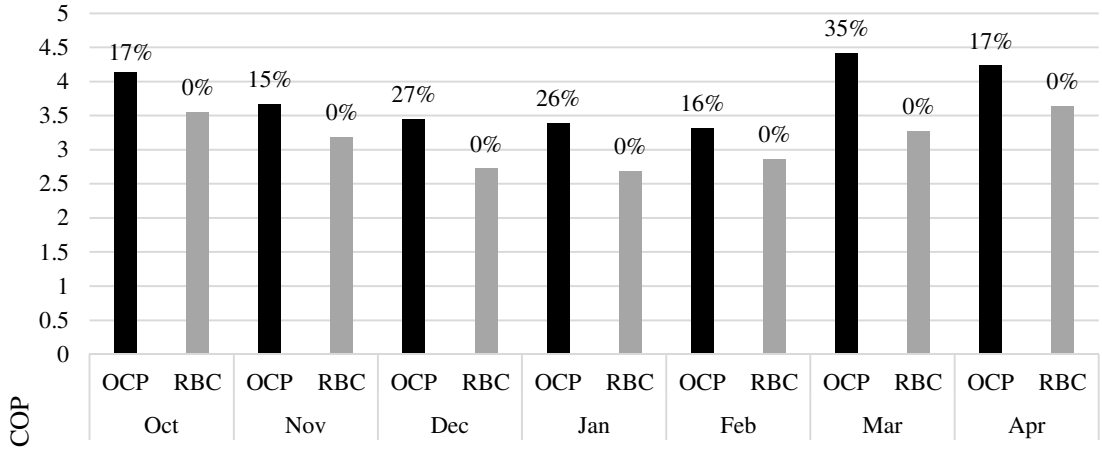

Figure 14 monthly AS-HP average COP: OCPs vs RBC

In fact looking at Figure 14, the OCP solution uses the AS-HP in a more efficient way, with an average $COP_{OCPs,Win}$ = 3.46 in Winter and $COP_{OCPs,A\text{-}S}$ = 4.26 in Autumn and Spring, with respect to the RBC $COP_{RBC,Win}$=2.86 in Winter and $COP_{RBC,A\text{-}S}$ = 3.48 in Autumn and Spring. To summarize the figures above the OCP is able to better exploit the hybrid heating system, using the HP in a more efficient way with respect to the RBC, since the COP affects the electrical power absorbed by the HP and thus the cost of electricity per kWh generated while using the HP.

4.2 Comparison of optimal strategy and RBC for two sample months

In this section the detailed results for January and April are reported, highlighting the thermal comfort and the integration between the heating system operation and the photovoltaic system.

In Figure 15 and Figure 16, the room temperatures T_r profiles of the OCPs and the RBC are plotted against the thermal comfort band, and the occupation heat gain to identify the occupied period. The days considered go from Thursday to Monday of a sample week for January and April on the x-axis for all the time plots.

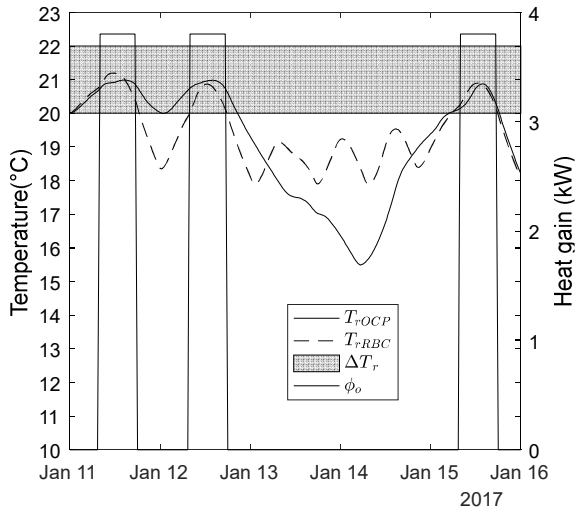

Figure 15 , T_r against ϕ_o, RBC (dashed line) vs OCPs (solid line), January

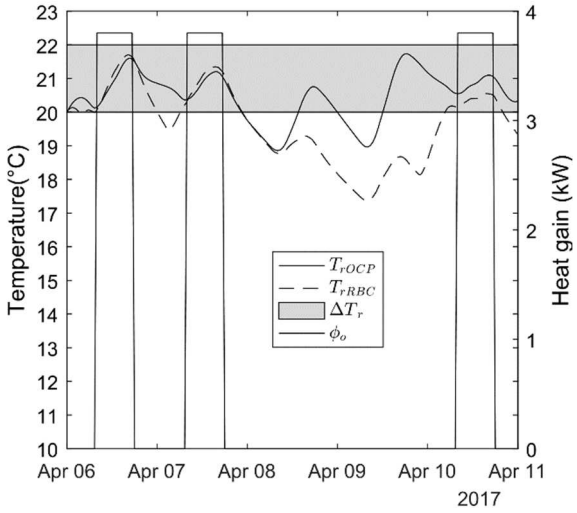

Figure 16. T_r against ϕ_o, RBC (dashed line) vs OCPs (solid line), April

Both in January and April, T_r profiles obtained by the OCPs are comparable with the temperature profiles obtained by the RBC in the occupied period, meaning that the rule-based controller has been properly tuned to achieve thermal comfort.

However, during January, the RBC must keep a proper set-back temperature T_r = 18 (°C) to achieve thermal comfort after the weekend on Monday, since nobody is present during Saturday and Sunday. This brings

wasteful consumption of energy that could be avoided when implementing the OCPs, since it is able to use the weather forecasts to predict the building temperature drop that will occur during the weekend and start the heating system in time to achieve thermal comfort on Monday.

During April, as expected the OCPs warms the building beforehand discharging the TES, and charging it back converting the excess energy produced by the PVs into thermal energy using the AS-HP, while the RBC mainly sells the PVs excess energy to the grid. In fact, looking at Figure 17 the total self-consumption factor for the OCPs (continuous line) is 0.98 and the total self-consumption factor for the RBC (dashed line) is 0.67. The self-consumption factor is calculated as:

$$SCF = \int_{t_0}^{t_f} \frac{\Delta P_{PVs}}{P_{PVs}} dt = \int_{t_0}^{t_f} \left(1 - \frac{\left(P_{PVs} - P_{build} - P_{elhp}\right)^{+}}{P_{PVs}}\right) dt \quad (23)$$

where ΔP_{PVs} is net the electrical power output of the PVs that is sold to the grid.

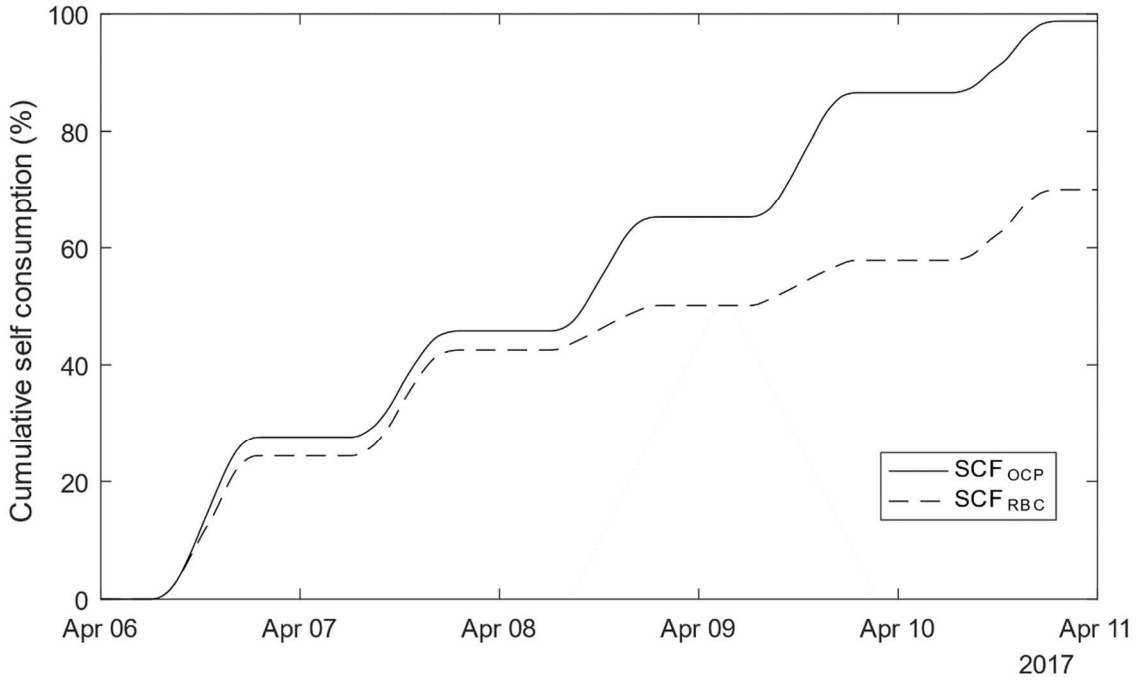

Figure 17 Cumulative PVs self-consumption factor for April: OCPs vs RBC

The increase in self-consumption is due to the difference between the average electricity price p_{el}=0.167 (€/kWh) and the contribution $p_{feed_{in}} = 0.08$ (€/kWh) for selling energy to the grid, which means it is more economically convenient to convert the PVs electricity into thermal energy and store it into the building

rather than selling it to the power grid and buy electricity at a higher price later from the grid to run the AS-HP.

In Figure 18 are reported Electrical power inputs of the AS-HP P_{elhp} (black lines, continuous line for the OCP and dashed line for the RBC), against the excess power output of the photovoltaic $\Delta P_{PVs\text{-}build}$ (red line), where $\Delta P_{PVs\text{-}build}$ is the power output of the *PVs* minus the building electrical consumption for other utilities as shown in Figure 5.

$$\Delta P_{PVs-build} = (P_{PVs} - P_{build})^{+} \tag{24}$$

The plot is reported only for April since in January the contribution from PVs is negligible due to low solar radiation.

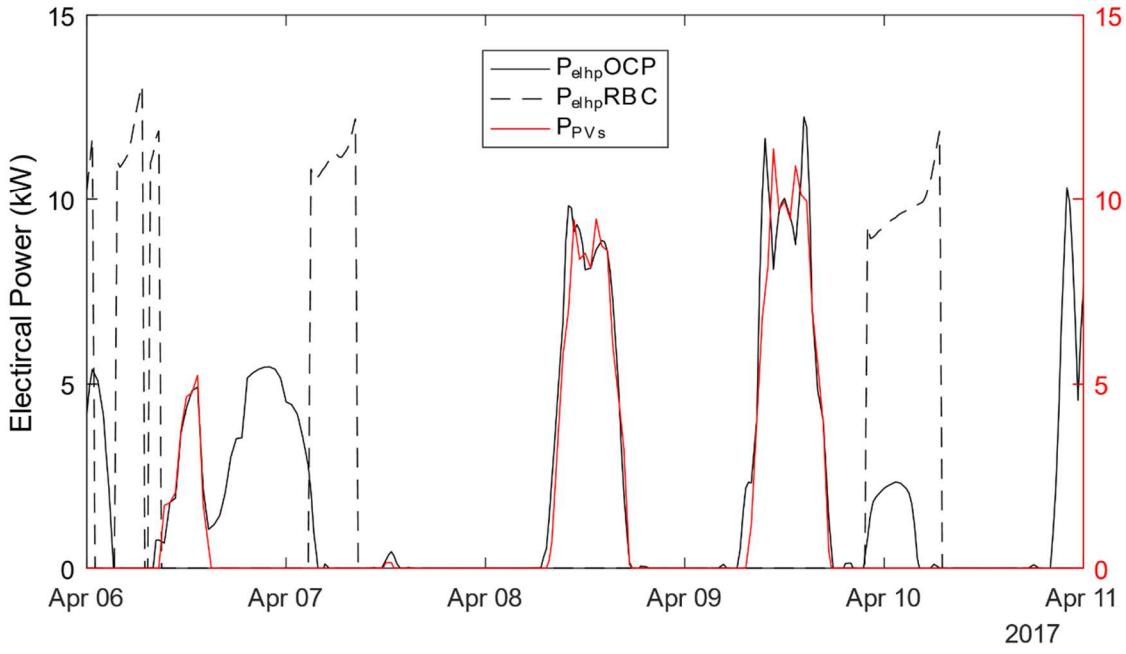

Figure 18 P_{elhp} against the excess ΔP_{PVs}: OCPs vs RBC

Looking at Figure 18 the OCPs operates the AS-HP so that the power input profile P_{elhp} OCPs follows the power output $\Delta P_{PVs-build}$ by modulating the AS-HP at partial load reducing its outlet temperature to maximize the SCF as shown before.

5. Conclusions

Considering thermal comfort, the results of the Rule Based Controller (RBC) and the Optimal Control Problem solution (OCPs) are comparable, meaning that the RBC was properly tuned for this simulation,

485 however in real-time applications it is not easy to finely tune RBCs, leading typically to worse thermal
486 comfort results. The same can be said also for the total heat input in the building Q_{tot}, however the OCPs
487 outperforms the RBC achieving energy consumption cost savings on average around 20%. Even from an
488 environmental perspective the results are encouraging, with average avoided CO_2 emissions $\Delta E_{CO_2} = 10\%$.
489 This means that the OCPs is using the hybrid heating system in a more efficient way with respect to the
490 RBC fully exploiting the presence of the Thermal Energy Storage (TES) and the photovoltaic system (PVs).
491 In fact, the OCPs increases the PVs self-consumption to almost 100% from 67% of the RBC.
492 In the colder months the OCPs switches between the Air Source Heat Pump (AS-HP) and the gas boiler
493 depending on which one is the cheapest option. In Autumn and Spring, the OCPs prioritizes the AS-HP
494 exploiting the decoupling offered by the TES to spread the demand and to store the excess energy produced
495 by the PVs promoting self-consumption and achieve the goal of a nearly zero energy building.
496 In this work was confirmed the potential of advanced control techniques for complex building
497 frameworks such as in NZEBs buildings. In a real case application, the performance of the control system
498 will be affected by the accuracy of the weather forecasts and the constraints on the technologies adopted
499 which in some cases are not designed to have variable set-points as derived from the OCP solution, therefore
500 a post processing phase is needed reducing the optimization gain. However, having 20% theoretical
501 economic savings with respect to a well-tailored RBC is a promising margin for future experimental works.
502 The validation of these models and results will occur in future studies considering the same building or
503 similar buildings in the North Italian scenario.

504 **Acknowledgements**

505 This study was carried out as master thesis collaboration between Politecnico of Milano Department of
506 Energy and Korean Advanced Institute of Science and Technologies (KAIST) Cho Chun Shik Graduate
507 School for Green Transportation.

508

509 **References**

510 [1] Eurostat, "Eurostat:Consumption of energy," 2016. [Online]. Available:
511 http://ec.europa.eu/eurostat/statistics-explained/index.php/Consumption_of_energy.
512 [2] M. Economidou, J. Laustsen, P. Ruyssevelt, and D. Staniaszek, "Europe ' S Buildings Under the

Microscope," 2011.

[3] D. Kolokotsa, D. Rovas, E. Kosmatopoulos, and K. Kalaitzakis, "A roadmap towards intelligent net zero- and positive-energy buildings," *Sol. Energy*, vol. 85, no. 12, pp. 3067–3084, 2011.

[4] I. Sartori, A. Napolitano, and K. Voss, "Net zero energy buildings: A consistent definition framework," *Energy Build.*, vol. 48, pp. 220–232, 2012.

[5] M. Kapsalaki, V. Leal, and M. Santamouris, "A methodology for economic efficient design of Net Zero Energy Buildings," *Energy Build.*, vol. 55, pp. 765–778, 2012.

[6] European Comission, *Horizon 2020 Work Programme 2018 - 2020: 10. Secure, Clean and Efficient Energy*, no. October 2017. 2017, p. 198.

[7] D. D'Agostino, P. Zangheri, and L. Castellazzi, "Towards nearly zero energy buildings in Europe: A focus on retrofit in non-residential buildings," *Energies*, vol. 10, no. 1, 2017.

[8] E. Union, *Directive 2009/28/EC*. 2009.

[9] I. Government, *Decreto Legge 83del 22.6.2012*. .

[10] C. Candelise, M. Winskel, and R. J. K. Gross, "The dynamics of solar PV costs and prices as a challenge for technology forecasting," *Renew. Sustain. Energy Rev.*, vol. 26, pp. 96–107, Oct. 2013.

[11] G. Li, "Parallel loop configuration for hybrid heat pump – gas fired water heater system with smart control strategy," *Appl. Therm. Eng.*, vol. 138, pp. 807–818, Jun. 2018.

[12] C. Di Perna, G. Magri, G. Giuliani, and G. Serenelli, "Experimental assessment and dynamic analysis of a hybrid generator composed of an air source heat pump coupled with a condensing gas boiler in a residential building," *Appl. Therm. Eng.*, vol. 76, pp. 86–97, Feb. 2015.

[13] G. Bagarella, R. Lazzarin, and M. Noro, "Annual simulation, energy and economic analysis of hybrid heat pump systems for residential buildings," *Appl. Therm. Eng.*, vol. 99, pp. 485–494, Apr. 2016.

[14] D. Fischer and H. Madani, "On heat pumps in smart grids: A review," *Renew. Sustain. Energy Rev.*, vol. 70, no. May 2016, pp. 342–357, 2017.

[15] D. Fischer, J. Bernhardt, H. Madani, and C. Wittwer, "Comparison of control approaches for variable speed air source heat pumps considering time variable electricity prices and PV," *Appl. Energy*, vol. 204, pp. 93–105, 2017.

[16] H. Thieblemont, F. Haghighat, R. Ooka, and A. Moreau, "Predictive control strategies based on

weather forecast in buildings with energy storage system : A review of the state-of-the art," *Energy Build.*, vol. 153, pp. 485–500, 2017.

[17] M. W. Ahmad, M. Eftekhari, T. Steffen, and A. M. Danjuma, "Investigating the performance of a combined solar system with heat pump for houses," *Energy Build.*, vol. 63, pp. 138–146, 2013.

[18] R. Halvgaard *et al.*, "Model predictive control for a smart solar tank based on weather and consumption forecasts," *Energy Procedia*, vol. 30, pp. 270–278, 2012.

[19] I. Hazyuk, C. Ghiaus, and D. Penhouet, "Model Predictive Control of thermal comfort as a benchmark for controller performance," *Autom. Constr.*, vol. 43, pp. 98–109, 2014.

[20] S. Li, J. Joe, J. Hu, and P. Karava, "System identification and model-predictive control of office buildings with integrated photovoltaic-thermal collectors, radiant floor heating and active thermal storage," *Sol. Energy*, vol. 113, pp. 139–157, 2015.

[21] Z. Du, X. Jin, X. Fang, and B. Fan, "A dual-benchmark based energy analysis method to evaluate control strategies for building HVAC systems," *Appl. Energy*, vol. 183, pp. 700–714, Dec. 2016.

[22] A. Parisio, L. Fabietti, M. Molinari, D. Varagnolo, and K. H. Johansson, "Control of HVAC Systems via Scenario-based Explicit MPC," pp. 5201–5207, 2014.

[23] F. Amara, K. Agbossou, A. Cardenas, Y. Dubé, and S. Kelouwani, "Comparison and Simulation of Building Thermal Models for Effective Energy Management," *Smart Grid Renew. Energy*, vol. 06, no. 04, pp. 95–112, 2015.

[24] 1975. Print University of Wisconsin--Madison. Solar Energy Laboratory. Wis. :The Laboratory, "TRNSYS, a Transient Simulation Program." .

[25] D. B. Crawley *et al.*, "EnergyPlus: Energy Simulation Program," *ASHRAE J.*, vol. 42, no. 4, pp. 49–56, 2000.

[26] E. Zavaglio, R. Scoccia, and M. Motta, "RC building modelling for control purposes : a case study," in *BSA 2017 Proceeding Book*, 2017.

[27] R. Lombardia, "www.arpalombardia.it," 2015. [Online]. Available: http://www.arpalombardia.it/Pages/ARPA_Home_Page.aspx.

[28] C. Delmastro, G. Mutani, and S. Perassi, "In Use Monitoring of Public Buildings . Case Study in North Italy," *Int. J. Heat Technol.*, vol. 34, no. 2, pp. 266–276, 2016.

569 [29] E. M. Kleinbach, “Performance Study of One-Dimensional Models for Stratified Thermal Storage
570 Tank by Master of Science University of Wisconsin-Madison,” vol. 50, no. 2, pp. 155–166, 1990.
571 [30] C. Verhelst, F. Logist, J. Van Impe, and L. Helsen, “Study of the optimal control problem formulation
572 for air-to-water heat pump systems,” *KU Leuven*, pp. 43–46, 2012.
573 [31] GSE, “Electricity and Natural gas prices.” [Online]. Available: http://www.mercatoelettrico.org/it/.
574 [32] P. Falugi, E. Kerrigan, and E. Van Wyk, “Imperial College London Optimal Control Software User
575 Guide (ICLOCS).” _Department of Electrical and Electronic Engineering, Imperial College London
576 London England, UK, pp. 1–86, 2010.
577 [33] I. The MathWorks, “MATLAB 2015b.” Natick, Massachusetts, United States.
578 [34] B. Bialeckit, G. Fairweathert, and K. R. Bennett, “FAST DIRECT SOLVERS FOR PIECEWISE
579 HERMITE BICUBIC ORTHOGONAL SPLINE COLLOCATION EQUATIONS,” vol. 29, no. 1, pp.
580 156–173, 1992.
581 [35] A. Wächter and L. T. Biegler, “On the implementation of a primal-dual interior point filter line search
582 algorithm for large-scale nonlinear programming (IPOPT),” vol. 57. pp. 25–26, 2004.